Journal of Materials Chemistry C

Exceptional Electromagnetic Shielding Efficiency of Silver Coated Carbon Fiber Fabrics via Roll-to-Roll Spray Coating Process

Journal:	*Journal of Materials Chemistry C*
Manuscript ID	TC-ART-04-2020-002048.R1
Article Type:	Paper
Date Submitted by the Author:	05-Jun-2020
Complete List of Authors:	Park, Janghoon; University of Massachusetts Amherst, Polymer science and engineering Hu, Xiyu; University of Massachusetts Amherst, Polymer science and engineering Torfeh, Mahsa; University of Massachusetts Amherst, Electrical and Computer Engineering Okoroanyanwu, Uzodinma; University of Massachusetts Amherst, Polymer science and engineering Arbabi, Amir; University of Massachusetts Amherst, Electrical and Computer Engineering Watkins, James J.; University of Massachusetts Amherst, Polymer Science and Engineering

Exceptional Electromagnetic Shielding Efficiency of Silver Coated Carbon Fiber Fabrics via Roll-to-Roll Spray Coating Process

Janghoon Park[1,†], Xiyu Hu[1,†], Mahsa Torfeh[2], Uzodinma Okoroanyanwu[1], Amir Arbabi[2,], and James J. Watkins[1,*]*

[1]Department of Polymer Science and Engineering, University of Massachusetts Amherst, 120 Governors Drive, Amherst, MA, 01003, USA

[2]Department of Electrical and Computer Engineering, University of Massachusetts Amherst, 151 Holdsworth Way, Amherst, MA, 01003, USA

[*]*Corresponding author: arbabi@ecs.umass.edu (A.A.)*

watkins@polysci.umass.edu (J.J.W.)

Abstract

We report exceptionally high electromagnetic interference (EMI) shielding effectiveness (SE) for flexible weaved carbon fiber fabrics (CFFs), which were spray-coated with Ag nanoparticle ink without surface modification of CFFs substrate. CFFs spray coated with Ag on a roll-to-roll (R2R) platform with a total composite thickness of 460 μm exhibited remarkable EMI SE of 102 dB, with a density of 0.52 g/cm^3. The specific EMI SE and absolute EMI SE obtained were 194 dB·cm^3/g and 4266 dB·cm^2/g, respectively. These results suggest that R2R spray coating of conductive metal inks such as Ag on CFFs is an economical, promising, and scalable approach for manufacturing fabrics with exceptional EMI SE.

Kewords: *electromagnetic interference shielding, carbon fiber fabrics, silver nanoparticles, spray coating, roll-to-roll*

1. Introduction

The proliferation of electronic devices and wireless communication has greatly increased the risk of electromagnetic interference (EMI) between electromagnetic signals from these devices. At frequencies such as 2 GHz used in mobile phones, and 8-12 GHz used in radar, avionics and wireless computer networks, electromagnetic radiations can interfere with electronic devices and can also be harmful to human health.[1] Consequently, there is a significant interest in developing materials that can shield the electromagnetic waves emitted from electronic devices.

Generally, materials with good electrical conductivity have good EMI shielding performance.[2] For example, metals such as copper, nickel and aluminum with excellent conductivity have high EMI shielding effectiveness (SE).[3] However, because metals have finite conductivity, part of the electromagnetic radiation can be transmitted through thin metallic shields, and this reduces their SE.[4] In addition, for certain applications such as in avionics and flexible electronics, besides having excellent electrical conductivity, the shielding material needs to be lightweight and flexible. For these reasons, carbon-based materials have become attractive substitutions for metals in EMI shielding applications.[5-10] For instance, it has been reported that graphene has the potential to be an excellent EMI shielding material with specific SE (SSE) up to 500 dB·cm^3/g.[5] Moglie *et al.* achieved a SE of 40 dB by using carbon foams.[11] Zeng *et al.* prepared a composite of multi-walled carbon nanotubes and waterborne polyurethane with a SE of 51 dB.[12] Li *et al.* fabricated a composite of polyimide and reduced graphene oxide, which had a SE of 21 dB.[13] A graphene and carbon nanotube based composite also showed good performance of 75 dB for shielding.[14] Xing *et al.* reported an ultra-thin and flexible carbon-fabric/Ag/waterborne polyurethane film, which

exibit 102.9 dB.[15] Furthermore, 2D metal carbides (MXenes) have attracted great interest due to their excellent EMI SE of 40 dB at a thickness of 8-9 μm with 60 wt% of MXene loading.[2]

The processes for manufacturing the carbon-based shielding materials described above are complex and energy-intensive, which present difficulties in scaling them to high-volume manufacturing. Other simple method such as spray-style deposition has been widely utilized. For example, Liu and Kang reported a result of 80.82 dB within 900-1500 MHz range by spray coating two different solutions to initiate an oxidation-reduction reaction in situ on a non-woven carbon fiber fabric substrate.[16] These types of conductive fabrics have the advantages of high conductivity, flexibility, and stretchability, making them suitable for use as a base substrate for EMI shielding composite compared to non-conductive polymer substrates. Currently, advanced materials such as graphene-based fibers are expected to be utilized in wearable devices as well as EMI shielding films with remarkable electrical conductivity, tensile strength, and stretchability.[17-19]

We propose a simple and straightforward method by spray coating to fabricate Ag/carbon fiber fabrics (CFFs) composites, which has exceptional electromagnetic shielding efficiency within X-band (8-12 GHz) range. This process is available to the roll-to-roll (R2R) platform; thus a higher efficiency of manufacturing could be realized for continuous fabrication of Ag coated CFFs. We used CFFs as a substitute for polymers and conductive foams. To boost the EMI shielding of CFFs, we spray coated CFFs with Ag nanoparticle ink. In addition to high conductivity, Ag possesses attractive properties such as corrosion stability and applicability to a wide range of temperature, which collectively make it a suitable choice for EMI shielding applications.[20] Compared with the previous results in the literature,[21-26] our Ag coated CFFs showed the highest EMI SE of 102 dB.

2. Experimental

2.1 Materials

Ag nanoparticle ink (Metalon™ JS-B25HV), with particle size ranging from 60 to 80 nm, Ag content of 25%, viscosity of 10 mPa·s, surface tension of 32 mN/m was purchased from Novacentrix Co., Ltd., USA, and used as received without dilution or modification. The manufacturer's quoted resistivity and sheet resistance values for this ink following sintering were 2.8 μΩ·cm and 50 mΩ/□, respectively. CFFs with width of 76.2 mm and length of 9.2 m was purchased as rolls from Fibre Glast Co., Ltd., USA. The tensile strength, tensile modulus, elongation, and weight of the fabrics were 3.5–4.4 GPa, 227–240 GPa, 1.4–1.95%, and 13.5–14.7 mg/cm^2, respectively. The measured thickness was 221 μm.

2.2 Spray coating

Spray coating was performed in two modes: with a hand-held sprayer inside a fume hood and on a R2R platform. For safety reasons, the spray coating was carried out in an enclosed chamber, with exhaust lines and operated at negative pressure. The hand-held spray coater (CM-CP2, Anest Iwata Inc., Japan) had a nozzle diameter of 0.23 mm, capacity of 7 mL, and driven with an air pressure within the range of 0.1-0.29 MPa. The amount of Ag nanoparticles deposited on CFFs was controlled to 5.1, 6.5, and 17.5 mg/cm^2 by varying the spraying time. The deposited nanoparticles were sintered on a hot plate (PC 620D, Corning Inc., USA) at 300°C for 15 min after coating. Additional sintering in a furnace (Blue M, Thermo Fisher Scientific Inc., USA) at 300°C for 5 min was performed in order to ensure complete sintering.

For the R2R experiment, a general spray gun (DH580000AV, Campbell Hausfeld Co., Ltd., USA) with a larger capacity was used to ensure a sufficient coating times. The capacity of the container and the nozzle diameter were 591 mL and 1.4 mm, respectively. The deposited amount of Ag nanoparticles on a CFFs web was controlled by the speed of the web in a R2R system (Frontier Co., Ltd., USA), and a coating of 4 mg/cm^2 was obtained when the web speed was 1.54 m/min. The substrates were spray coated on the R2R platform with the Ag nanoparticle ink at a pressure of 0.24 MPa and at a coating distance of 15 cm (distance between the nozzle and substrate), following which the substrate was dried in a 3.6 m inline hot-air dryer at a temperature of 120°C, and then further dried with far-infrared radiation (at 30% power). Then the dried coated film was further sintered at a temperature of 300°C for 15 min.

2.3 Characterizations

The X-ray diffraction (XRD) spectra used to identify the crystal phases of Ag nanoparticles on the CFFs substrate were obtained using a PANalytical X'Pert XRD (Malvern Panalytical Co., Ltd., UK) with Cu Kα radiation (λ = 0.154 nm) at a scanning rate of 0.06°/min from 10° to 80°. The microstructures of all the CFFs samples were confirmed using a scanning electron microscopy (SEM) (Magellan 400 XHR-SEM, FEI Co., Ltd., USA) at an accelerating voltage of 3 kV. The sheet resistance was measured with a 4-point probe system (Pro-4, Signatone Co., Ltd., USA) with a source meter (2400 Keithley, Tektronix Inc., USA), by applying a current of 50 mA and the results were reported as the average values of ten repeated measurements for each group. The thickness of the composite was measured with an electronic thickness gauge (Model 547-526S, Mitutoyo Co., Ltd., Japan). Ten points were randomly measured, and the mean value was used.

Electrical conductivity was calculated based on repeated measurements of sheet resistance and thickness data, using the following Eq. (1),[27]

$$\sigma_c = \frac{1}{R_s t} \qquad (1)$$

Where σ_c, R_s, and t are the conductivity, average sheet resistance, and average thickness, respectively.

The EMI SE of the CFFs samples was measured in the frequency range of 8–12 GHz (X-band), using a vector network analyzer (Fig. S1, E8362B PNA series, Agilent Technologies, Inc., USA). As shown in Fig. S1(a), a sample holder was assembled between two WR90 waveguides, and the sample was mounted inside its aperture. Typically, the sample holder's aperture and the sample have same size as the waveguide apertures (1.02×2.28 cm^2). This approach works well for dielectrics, but it has a remarkable error for highly conductive materials with large SE values. The reason is that the measurement for high conductive materials is sensitive to the gaps around the sample inside the aperture. As it is difficult to cut the samples with micrometer accuracy, we modified the sample holder by etching a larger aperture (1.69×2.95 cm^2) partially through the original sample holder (Fig. S1(b)). The sample can be mounted in this groove (Fig. S1(c)). Hence, the smaller aperture will shield the gaps and reduces the sensitivity to the errors in sample's dimensions. The depth of the large aperture, which was 0.5 mm, was selected to be as close as possible to the sample's thickness.

The dependence of EMI shielding on electrical conductivity is given by the following Eq. (2),[4, 28]

$$SE = 20t\sqrt{\pi f \mu_0 \mu_r \sigma_c}\log(e) + 10\log\left(\frac{\sigma_c}{32\pi\varepsilon_0\mu_r f}\right) \qquad (2)$$

where SE is the shielding effectiveness in dB, μ_r is relative permeability, f is the frequency, e is Euler's number and σ_c, ε_0 and t are conductivity, permittivity and thickness of the sample, respectively. For our samples, the composite materials are nonmagnetic with $\mu_r \approx 1$.[29,

[30]Accordingly, SE is a function of electrical conductivity, frequency, and thickness. Thus, ensuring the sample has high conductivity is important in improving the SE of the sample.

EMI SE is defined as the logarithmic ratio of incoming power and transmitted power.[31] Total SE (SE_T) is defined as

$$SE_T = SE_A + SE_R + SE_{MR} \qquad (3)$$

where SE_A, SE_R, and SE_{MR} are the shielding by absorption, reflection and multiple reflections, respectively. When the thickness of the shielding material is smaller than the skin depth, reflection of the electromagnetic (EM) wave occurs at multiple boundaries and therefore SE_{MR} should be considered. However, in a composite with high shielding effectiveness and thickness like the material used in this experiment, multiple reflections are negligible.[2, 32] Therefore, the influence on SE_{MR} was neglected in this experiment.

SE_A and SE_R can be expressed in terms of scattering parameters (S_{11}, S_{12}, S_{21}, S_{22}) obtained from a vector network analyzer as[32]

$$SE_A = 10\log\left(\frac{1-|S_{11}|^2}{|S_{12}|^2}\right) \qquad (4)$$

$$SE_R = 10\log\left(\frac{1}{1-|S_{11}|^2}\right) \qquad (5)$$

where scattering parameters, S_{ij} represents the transmission or reflection coefficient of the composite, where i is the port through which the EM wave radiation is received and j is the port through which the incident wave is transmitted. As our samples are reciprocal and symmetric, $S_{11} = S_{22}$ and $S_{12} = S_{21}$.

SSE was evaluated considering the density of shielding materials using the following equation[33]

$$Specific\ EMI\ SE = \frac{EMI\ SE}{\rho_m} \qquad (6)$$

where ρ_m is the density of the shielding material, and unit of the SSE is dB·cm^3/g. Furthermore, the ASE is defined by the following[34]

$$Absolute\ EMI\ SE = \frac{Specific\ EMI\ SE}{t} \qquad (7)$$

Finally, the anticorrosion test of the samples was performed by immersing the samples in tap water for up to 5 days,[35] after which, the samples were removed from the water and dried in air, before their EMI SE were remeasured.

3. Results and discussion

Spray coating is a technique for forming a thin layer on virtually any type of substrate (e.g., glass, metal, plastic, etc.) by discharging a solution with a high-pressure gas flow, resulting in exceptional of conformability for a high-speed coating technique. It can thus be readily adapted to the R2R continuous process to produce a large-area sample. Reale *et al.* has provided an excellent review of the spray coating technique.[36] Here, we emphasize only the main points. The process involves several independent steps, including liquid precursor atomization, inflight droplet evaporation, and impact on the substrate, where spreading, drying and adhesion of the liquid material take place. Atomization is the first step in the spray coating process, and it involves the conversion of a bulk liquid such as the nanoparticle ink used in this study into small droplets. The atomization process is controlled by the dynamic pressure of the gas used to force the liquid through a nozzle, the surface tension, and the viscous forces of the liquid. It occurs in two main

regimes: a primary atomization regime (near the nozzle) caused by high frictional shearing forces between the liquid and the high-velocity gas, which generates filaments and large droplets; a secondary atomization regime which breaks up the filaments further downstream. For low-viscosity liquids such as the ink used in this study, the deformation of the droplet is primarily determined by the Weber number (W_e), a dimensionless number representing the ratio of the aerodynamic forces and the stabilizing surface tension forces:[36]

$$W_e = \frac{\rho V^2 D}{\sigma} \qquad (8)$$

where ρ, V, D, and σ are the liquid density (kg/m^3), initial relative velocity between the gas and the liquid (m/s), initial diameter of the droplet (m), and surface tension of the droplet (N/m), respectively. The higher the W_e, the larger the deforming external pressure forces (which lead to droplet breakup) compared with the reforming surface tension forces (which favor droplet aggregation).[36] A high value of W_e is typically obtained with high efficiency atomization resulting in the generation of a large number of droplets that can be deposited on a specific coated area. Thus, a denser coating and a better droplet spreading can be obtained.[37]

In our experiments, we coated Ag nanoparticle ink on the CFFs substrate with a spray gun, as shown in Fig. 1(a). Since the liquid properties were fixed [ρ, D and σ were constants in equation (8)], to obtain a high value of W_e, thus a high efficiency atomization, the gas pressure, which was correlated with the V, was adjusted to the maximum pressure of 0.24 MPa to provide a uniform coating. Under this pressure condition, We is calculated as 352. As the nanoparticle solution used in the experiments had a size up to 80 nm, we observed nozzle clogging and non-uniform coating under low-pressure condition. We conducted our experiments under high-pressure gas flow regime to ensure good film uniformity under continuous coating operation.

Figure 1(b) shows XRD patterns of a CFFs substrate, as well as that of an Ag-nanoparticle-coated CFFs obtained with spray coating condition of 17.5 mg/cm^2. For pristine CFFs, there are two broad diffraction peaks at 26° and 43°, which correspond to (002) and (100) reflections of graphite planes, respectively.[38] For the Ag-nanoparticle-coated CFFs, four distinct diffraction peaks at 38.1°, 44.3°, 64.4°, and 77.7° can be attributed to (111), (200), (220), and (311) planes, respectively, confirming that the Ag nanoparticles are face centered cubic and crystalline in nature.[39] This XRD pattern shows that the CFFs is well covered with Ag material, and the inset of Fig. 1(b) also confirms the good coverage in terms of the color difference of the surface.

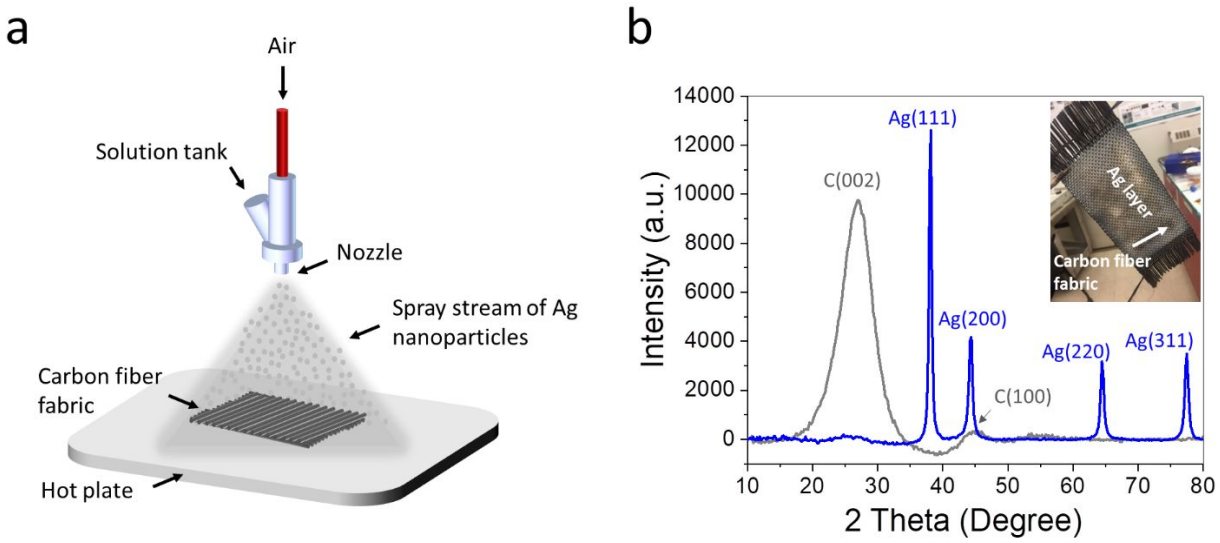

Fig. 1. (a) Fabrication of EMI shielding composite through spray coating of Ag nanoparticles onto CFFs substrate (b) XRD patterns of a CFFs and an Ag-nanoparticle-coated CFFs (inset photo of the measured Ag-coated CFFs).

Figure 2 shows the density and electrical conductivity of the Ag-coated CFFs. The Ag content, which depends on the spraying duration, are 5.1, 6.5, and 17.5 mg/cm^2, respectively. As the deposition amount increases, the areal density increases linearly from uncoated CFFs to 24.3, 25.7, and 36.7 mg/cm^2 [Fig. 2(a)]. However, the density values do not increase with the deposited

amount of Ag nanoparticles because there is an appreciable error uncertainty in the thickness of the CFFs substrate. Overall, coated samples showed a density range of 0.76–0.98 g/cm^3. The density value is a critical variable used in optimizing the performance of EMI shielding materials. Compared with recent publications, this composite shows a moderate level of EMI shielding performance based on density alone (see Table S1). Low-density structures including reduced graphene oxide, multi-walled or single-walled carbon nanotubes have been reported in the literature.[6, 12, 40] Although these structures may have a high SSE, the actual EMI SE may be low, and mass-producing them is fraught with a lot of challenges because of the use of complex fabrication process steps, such as chemical vapor deposition or vacuum filtration. In this respect, the use of CFFs in EMI shielding applications offers a significant advantage in terms of light weight when compared to other matrices such as polyimide, waterborne polyurethane, and polystyrene.[12, 31, 41]

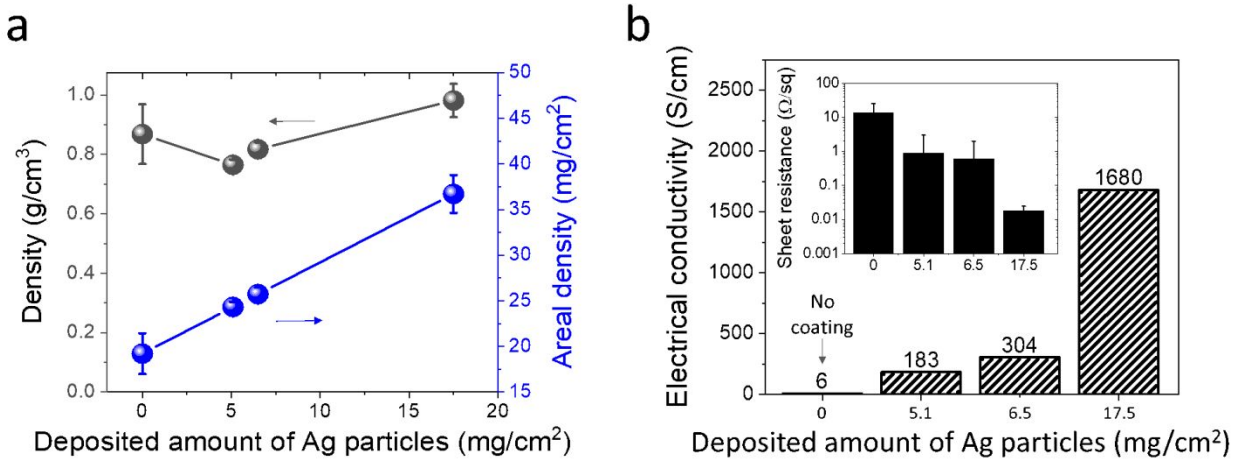

Fig. 2. Density and electrical conductivity of Ag-coated CFFs. (a) Density and areal density of the samples as a function of deposited amount of Ag nanoparticles during the spray process. The area of the measured sample was 1.69×2.95 cm^2 and the thickness value was 221–374 μm. (b) Electrical conductivity of the samples prepared by using different deposition amount of Ag nanoparticles (inset: sheet resistance data used for the electrical conductivity calculation).

The electrical conductivity according to the amount of Ag nanoparticles coating is shown in Fig. 2(b). The sheet resistance values for the uncoated CFFs sample and samples coated with Ag nanoparticles in the amounts of 5.1, 6.5, and 17.5 mg/cm^2 [inset of Fig. 2(b)] are 13.5±12.3, 0.9±2.1, 0.6±1.4, and 0.02±0.01 Ω/□, respectively. The thicknesses of the samples are 221±19, 318±20, 314±18, and 374±38 μm, respectively. The electrical conductivity of the samples shows a gradually increasing trend from the uncoated condition to the maximum amount of coating for 6, 183, 304, and 1680 S/cm, resulting in a maximum 279 times improvement. [Fig. 2(b)]. This value translate to exceptional performance for EMI shielding, which is comparable with the electrical conductivity of MXenes (1841 S/m with 80wt% of Ti_3C_2Tx filler contents).[2]

SEM images of CFFs are shown in Fig. 3(a-b). The plain weave pattern of the carbon fibers aids in ensuring high electrical conductivity of the CFFs. The diameter of a single fiber is approximately 8 μm, and the fibers are of a uniform size in the entire fabric network [Fig. 3(a)]. The SEM images of the 6.5, and 17.5 mg/cm^2 Ag coating conditions are shown in Fig. 3(c-f).

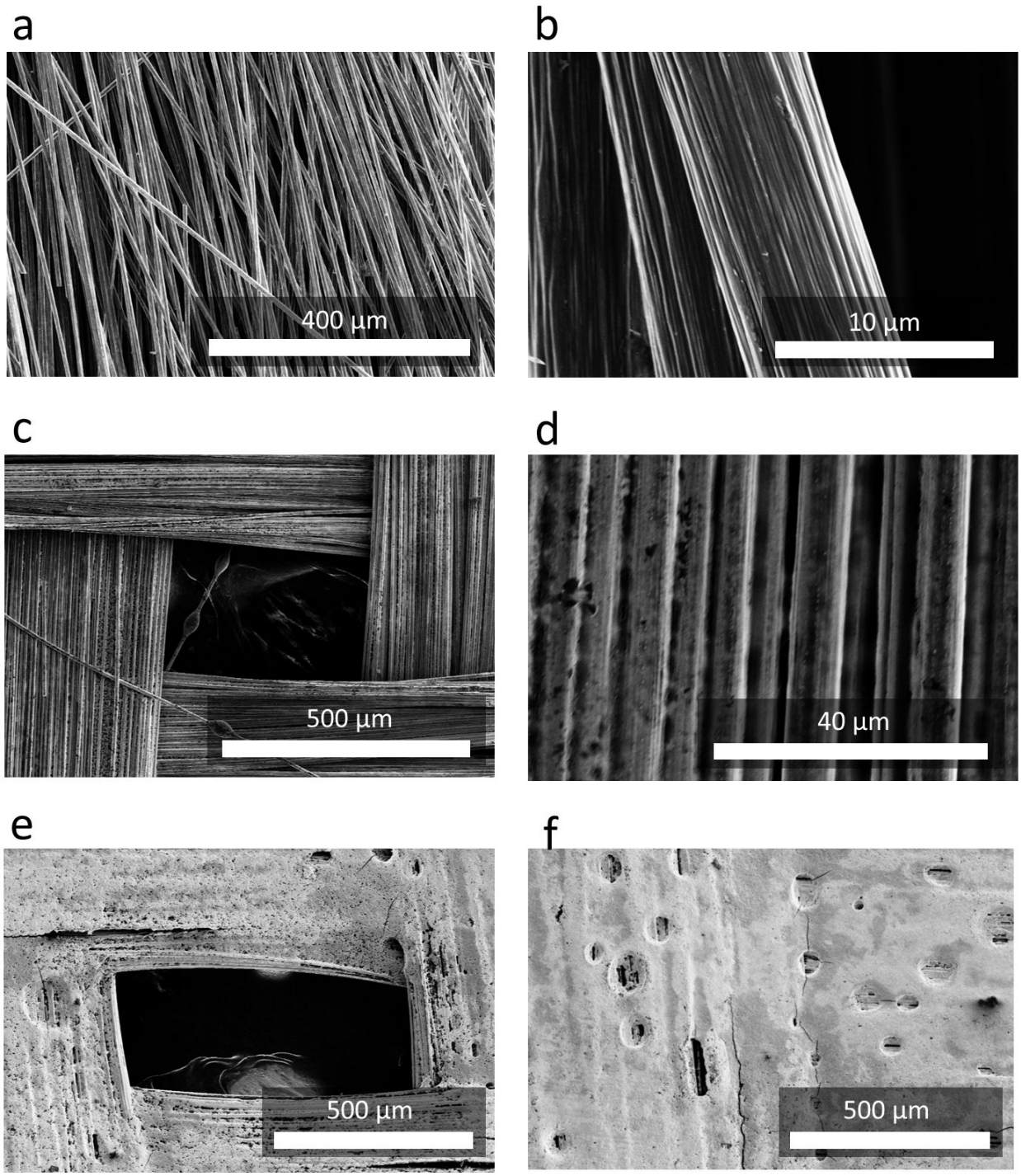

Fig. 3. SEM images of (a-b) a pristine CFFs substrate, (c-d) Ag coated CFFs with deposited amount of 6.5 mg/cm^2, and (e-f) 17.5 mg/cm^2.

Figure 3(c) shows that the Ag material adheres very well to the CFFs and is interconnected with the carbon fibers. From the magnified image shown in Fig. 3(d), the fibers are sufficiently bonded together with Ag nanoparticles after curing. This is very important from the viewpoint of EMI shielding, as the Ag coating can increase the electrical conductivity of fabric networks, as well as the reflection of the EM wave on the surface. The samples with the highest Ag coating in Fig. 3(e-f) shows that the Ag nanoparticles form a complete coverage layer over the CFFs substrate, which is a positive attribute in terms of electrical conductivity and SE, but may suffer from the drawback of being susceptible to bending or twisting in terms of mechanical robustness.

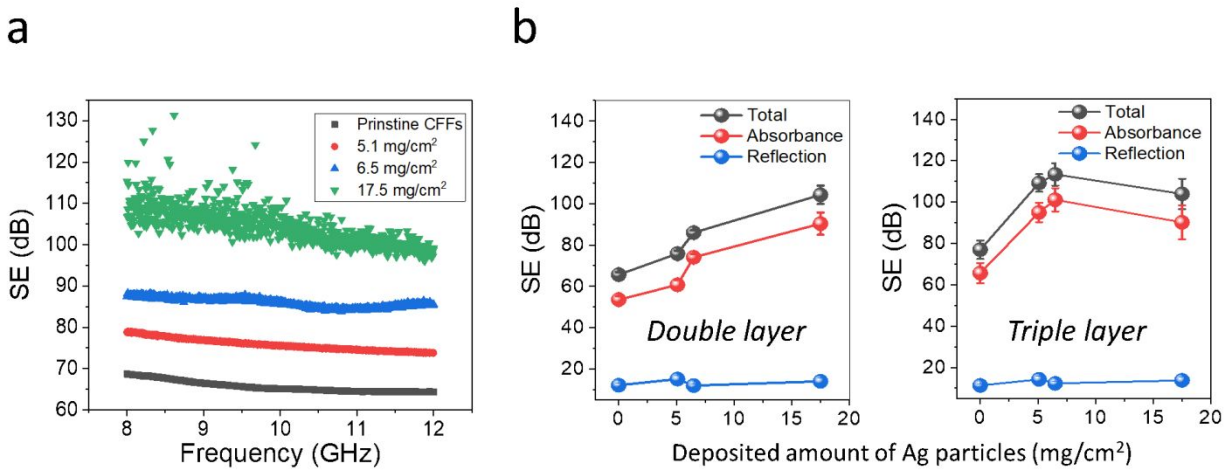

Fig. 4. EMI SE of Ag-coated CFFs. (a) SE of double-layer Ag-coated CFFs fabricated with pristine CFFs (no coating), 5.1, 6.5, and 17.5 mg/cm^2, (b) SE total (SE_T) and its absorption (SE_A) and reflection (SE_R) mechanism in Ag-coated CFFs with different amount of Ag nanoparticle coatings (left: double layer, right: triple layer).

Figure 4 shows the EMI SE of Ag spray-coated CFFs, measured in double and triple layers, over a thickness range of 440–750 μm and frequency range of 8 to 12 GHz. The SE was 66±1.1, 76±1.4, 86±1.3, and 104±4.5 dB, respectively, from uncoated pristine CFFs to samples Ag nanoparticles coated with 5.1, 6.5, and 17.5 mg/cm^2, respectively [Fig. 4(a)]. The neat CFFs itself shows a shielding efficiency of 66 dB. When CFFs is coated with Ag nanoparticles, the SE increases to a

maximum of 104 dB. This suggests that the EMI shielding performance increases with coating amount, given the increase in electrical conductivity resulting from the Ag nanoparticle. However, when the SE of a single layer of the composite is measured, the SE value does not increase appreciably with Ag content as shown in Fig. S2(a). Fig. S2(b) shows that this is because the leakage of EM waves through the openings in the weave pattern degrades the SE. However, for the double-layer sample, the overlapping patterns between the layers [see the cartoon on the right of Fig. S2(b)] were able to close these openings, ensuring low leakage of the EM waves through intervening layers and thus an increase in the observed SE.

Figure 4(b) shows SE_T, SE_A, and SE_R measurements of the double-layer and triple-layer samples (650–1200 μm thickness) as a function of Ag content. In the double-layer sample, reflection contributed 11-14 dB of the total EMI shielding effectiveness, while absorption contributed as much as 53–90 dB to the total EMI shielding effectiveness. This means that ~95% of the incident power is reflected, 5% of it enters the shielding material, and ~2.5×10^{-7}% passes through it. For the triple-layer sample, shielding by reflection also shows a similar value to that of the double-layer case (from 11 to 14 dB), and the shielding by absorption increases from 65 to 101 dB; it also increases as a function of the amount of Ag nanoparticles content (see Fig. S3 and S4 for the measured SE_T, SE_A, and SE_R). As it is displayed in Fig. 4, the measured shielding effectiveness of the triple-layer sample stays below 115 dB. This is because the setup has an SE measurement limit of ~110 dB and beyond that, the setup cannot provide an accurate result, as the transmitted signal is smaller than the system's noise.[42] Hence, the triple-layer sample might have provided more than 115 dB of shielding. Also, samples with high shielding effectiveness are more sensitive to holes and roughness; hence, the reduction in shielding effectiveness of the triple-layer sample with high amount of Ag might be due to its sensitivity to such imperfections.

The experiments described above show the possibility for the continuous fabrication of Ag-coated CFFs composites with the aid of R2R spray coating process. Figure 5(a) shows a schematic diagram of a process for R2R spray coating of Ag nanoparticle ink on a CFFs web. The R2R system consists of unwinding, in-feeding, coating, drying, out-feeding and rewinding parts [Fig. 5(b)]. Edge position controller and a load cell were used for R2R web lateral control and tension control. Figure 5(c) shows the process for coating the actual Ag nanoparticle ink on the CFFs web. The CFFs web (76.2 mm web wide and 9.2 m long) was transported by attaching the polyester web to the backside as the support substrate. Unlike the hand-held spray coating experiments, in which the CFFs substrate was coated at a specific distance manually, the R2R experiment was conducted at a speed of 1.54 m/min when the spray was applied, ensuring a more uniform coating, as shown in Fig. 5(d). The R2R spray-coated CFFs network was immediately dried at 120°C in a far-infrared drying oven, which was part of a 3.6 m long hot-air dryer. The web speed was 1.54 m/min and the drying time was 2.3 min. Sintering at a temperature of more than 300°C in the R2R inline process was not possible in this system. Therefore, the coated CFFs was sampled and sintered in an offline furnace. The deposited amount of Ag nanoparticles and density of the composite obtained were 4.05 mg/cm^2 and 0.52 g/cm^3, respectively. Finally, EMI SE of the R2R processed sample was 102±2.4 dB (double layer), as shown in Fig. 5(e). The measured values were superior to those obtained with the hand-held spray coater with a similar amount of coated Ag nanoparticles because the spray stream was uniformly deposited on the CFFs web while the web was transported at a constant speed. This can be seen indirectly through the excellent uniformity of the Ag-coating on the sample shown in Fig. 5(d).

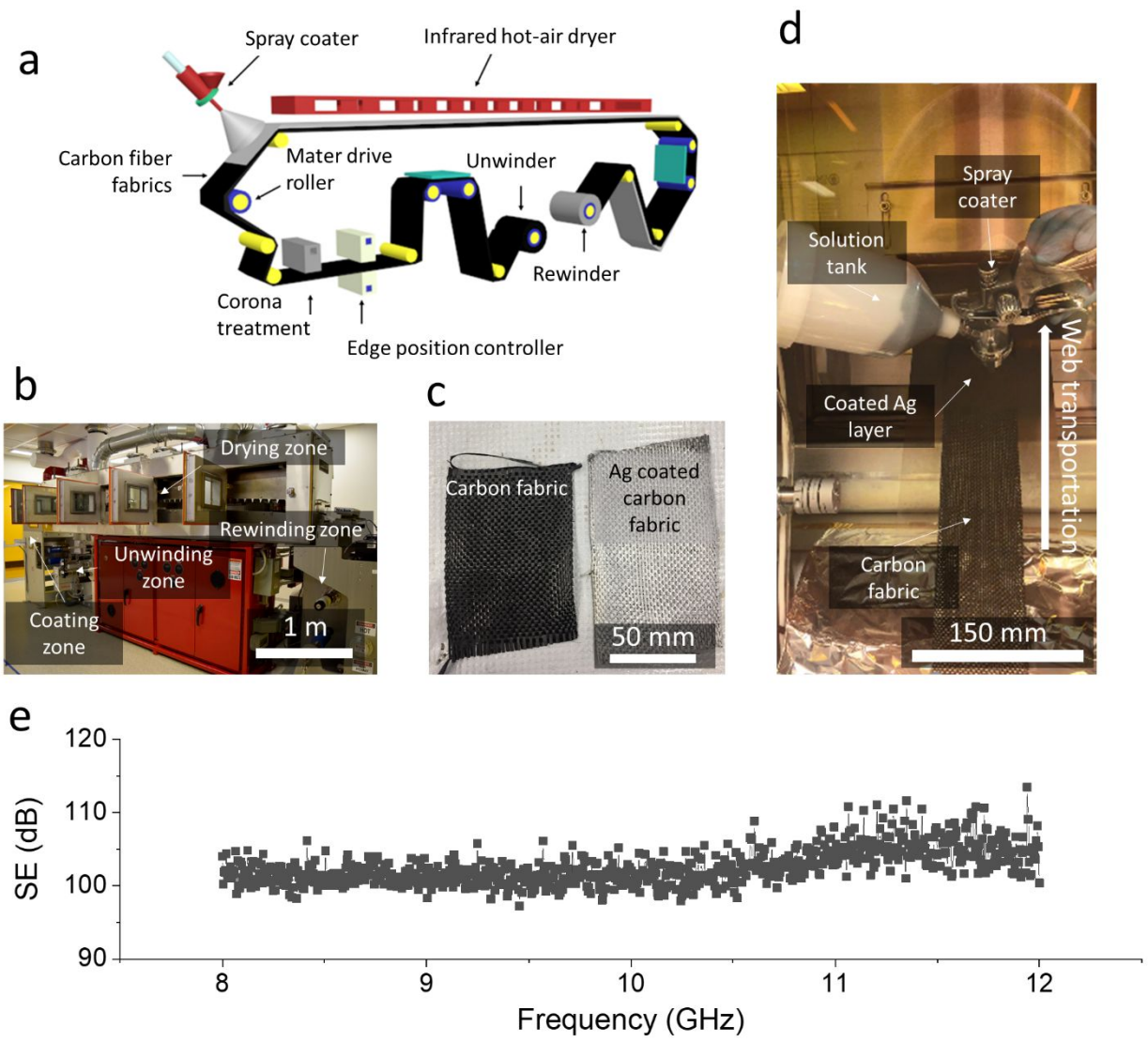

Fig. 5. Manufacture of R2R Ag-coated CFFs composite. (a) A schematic of the R2R Ag nanoparticle ink coating process onto CFFs web substrate, (b) the R2R platform used in the experiment, (c) A photograph of the a piece of CFF and an Ag coated CFF, (d) A photograph of the spray coating of Ag nanoparticle ink during transfer of the CFFs web substrate, (e) EMI SE measurement result of the prepared Ag coated CFFs.

An anticorrosion test[35] for the R2R Ag coated CFFs composite was performed as shown in Fig. 6. The composite was immersed in tap water for up to 5 days and evaluated for electrical conductivity and EMI SE. Figure 6(a) compares the SE of the sample immediately after R2R processing and the sample after 5 days of immersion in tap water. Each sample shows an SE of 102±2.5 and

89±1.9 dB, SE difference of 13 dB, which is not large as shown in Fig. 6(b). However, the composite was observed to have slowly degraded in tap water (see Fig. S5 for the measured SE of anticorrosion tested samples). This is because the Ag material was slowly oxidized in the tap water and the atmosphere,[43] therefore, lamination of the prepared composite is needed, just as is done on solar cell devices to ensure stability.[44] In other respects, however, the stability of this composite is acceptable when comparing its resistance values with the anticorrosion data of Cu films in the literature.[35] Figure 6(c) shows the resistance change (R/R_0) during anticorrosion test in tap water, where R is the measured resistance and R_0 is the initial resistance value, i.e., the pristine sample. The Ag coated CFFs sample showed a resistance increase of up to 1.17 times in the tap water test and showed excellent stability, but the Cu film shows an increase in resistance up to 6 times and was very quickly oxidized in tap water.

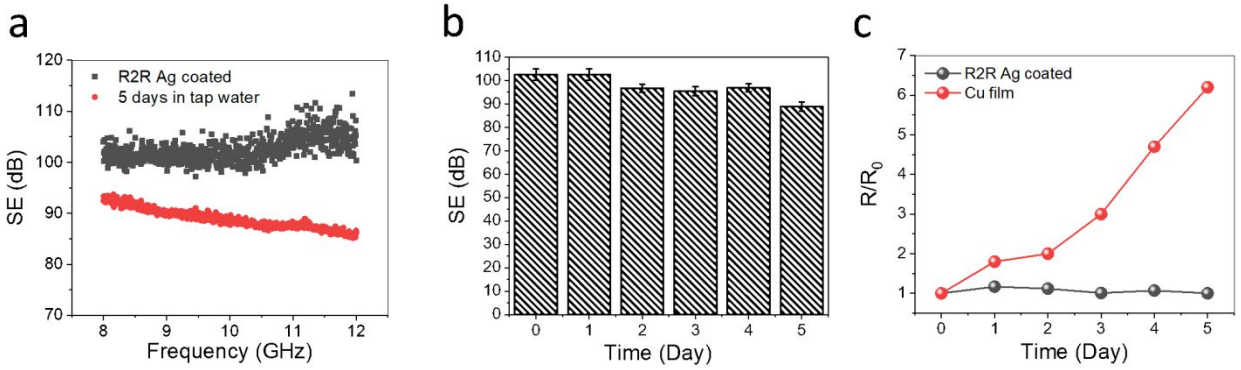

Fig. 6. Anticorrosion test of Ag coated CFFs composite. (a) SE comparison between the R2R Ag-coated CFFs and Ag-coated CFFs immersed in tap water for 5 days, (b) SE change of Ag coated CFFs as immersion times in tap water from 0 to 5 days, and (c) Resistance change of the fabricated composites and Cu films.[35]

Figure 7 indicates the comparison of the EMI SE, SSE, and ASE between the fabricated Ag-coated CFFs composites and previous studies.[2, 6, 11, 45, 46]

Compared with the previously reported values in the literature (see Table S1 for the listed survey data of Fig. 7), the fabricated-Ag coated CFFs showed highest EMI SE as shown in Fig. 7(a). The maximum EMI SE obtained was 104 dB for a CFFs coated with Ag content of 21 wt% and a thickness of 636 µm via hand-held spray coater. In contrast, the CFFs coated with 17 wt% of Ag to the thickness of 455 µm in the R2R platform showed a SE of 102 dB. However, a representative example with a comparable thickness like the composite of the present study was obtained with an MXenes ($Ti_3C_2T_x$), which showed an EMI SE performance of 68 dB at a thickness of 11 µm.[2] The fabricated Ag coated CFFs have a moderate SSE of 77–194 dB·cm^3/g and ASE of 4266 dB·cm^2/g compared to previous studies,[12, 47-49] as shown in Fig. 7(b). In contrast to the results reported in the literature, whose EMI SE performance can be attributed to bulk metals such as Al foil[45] or are manufactured with complex and energy-intensive methods that are not amenable to high-speed large-area processing such as electrospinning, chemical vapor deposition and freeze-drying techniques,[12, 50, 51] the spray coating process reported in this work for depositing Ag on CFFs yields high EMI SE values, is simple, fast, low-cost and is amenable to high-speed processing on large form factor substrates.

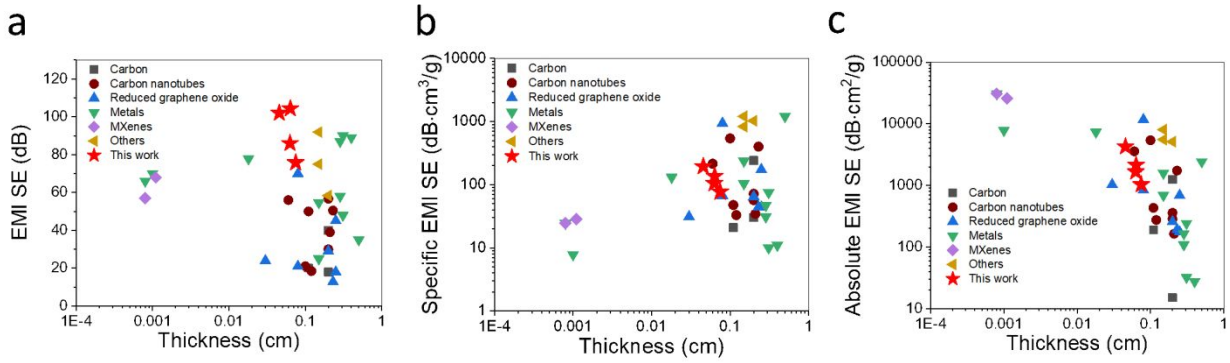

Fig. 7. (a) EMI SE, (b) specific EMI SE, and (c) absolute EMI SE of Ag-coated CFFs with the previous literature.

4. Conclusion

We have obtained a significant high EMI shielding performance for flexible weaved carbon fabrics spray-coated with Ag nanoparticle ink on a R2R platform. Total EMI SE, SSE and ASE results are comparable to the best performing lab-scale-based materials and processes previously reported in the literature in terms of thickness and density. With a total EMI SE, SSE and ASE of 102 dB, 194 dB·cm^3/g and 4266 dB·cm^2/g, respectively, all obtained on 460-μm-thick Ag-coated carbon fabric with a density of 0.52 g/cm^3, these results suggest that R2R spray coating of conductive metal inks such as Ag on CFFs substrates is an economical, promising, and scalable approach for manufacturing fabrics with exceptional EMI shielding effectiveness. In the future, it is expected that the metal deposition process based on these CFFs can be applied to various techniques such as magnetron sputtering[52] and electroless plating[53] as well as solution-based processes.

Article information

Notes

The authors declare no competing financial interest.

ORCID

Janghoon Park: 0000-0002-5897-4241

Xiyu Hu: 0000-0002-3362-9783

Author Contributions

[†]J.P. and X.H. contributed equally to this work.

Acknowledgments

This work was supported by the Army Research Laboratory (W911NF-15-2-0024). The facilities used in this work were supported by the Department of Polymer Science and Engineering, University of Massachusetts Amherst. The vector network analyzer used in this work was supported by Professor Amir Arbabi's group, University of Massachusetts Amherst.

References

1. W. Chen, J. Wang, B. Zhang, Q. Wu and X. Su, *Mater. Res. Express*, 2017, **4**, 126303.
2. F. Shahzad, M. Alhabeb, C. B. Hatter, B. Anasori, S. M. Hong, C. M. Koo and Y. Gogotsi, *Science*, 2016, **353**, 1137-1140.
3. X. P. Shui and D. D. L. Chung, *J Electron Mater*, 1997, **26**, 928-934.
4. M. Jaroszewski, S. Thomas and A. V. Rane, *Advanced Materials for Electromagnetic Shielding: Fundamentals, Properties, and Applications*, Wiley, 2018.
5. Z. P. Chen, C. Xu, C. Q. Ma, W. C. Ren and H. M. Cheng, *Adv Mater*, 2013, **25**, 1296-1300.
6. Y. L. Yang and M. C. Gupta, *Nano Lett*, 2005, **5**, 2131-2134.
7. H. B. Zhang, Q. Yan, W. G. Zheng, Z. X. He and Z. Z. Yu, *Acs Appl Mater Inter*, 2011, **3**, 918-924.
8. M. H. Al-Saleh, W. H. Saadeh and U. Sundararaj, *Carbon*, 2013, **60**, 146-156.
9. A. Chaudhary, S. Kumari, R. Kumar, S. Teotia, B. P. Singh, A. P. Singh, S. K. Dhawan and S. R. Dhakate, *Acs Appl Mater Inter*, 2016, **8**, 10600-10608.
10. J. Ling, W. Zhai, W. Feng, B. Shen, J. Zhang and W. g. Zheng, *Acs Appl Mater Inter*, 2013, **5**, 2677-2684.
11. F. Moglie, D. Micheli, S. Laurenzi, M. Marchetti and V. M. Primiani, *Carbon*, 2012, **50**, 1972-1980.
12. Z. Zeng, H. Jin, M. Chen, W. Li, L. Zhou and Z. Zhang, *Advanced Functional Materials*, 2016, **26**, 303-310.
13. Y. Li, X. L. Pei, B. Shen, W. T. Zhai, L. H. Zhang and W. G. Zheng, *Rsc Adv*, 2015, **5**, 24342-24351.
14. X. Y. Sun, X. Liu, X. Shen, Y. Wu, Z. Y. Wang and J. K. Kim, *Compos Part a-Appl S*, 2016, **85**, 199-206.
15. D. Xing, L. Lu, Y. Xie, Y. Tang and K. S. Teh, *Materials & Design*, 2020, **185**, 108227.

16. C. Liu and Z. Kang, *Appl Surf Sci*, 2019, **487**, 1245-1252.
17. F. Sun, M. Tian, X. Sun, T. Xu, X. Liu, S. Zhu, X. Zhang and L. Qu, *Nano letters*, 2019, **19**, 6592-6599.
18. X. Hu, M. Tian, T. Xu, X. Sun, B. Sun, C. Sun, X. Liu, X. Zhang and L. Qu, *ACS nano*, 2019.
19. M. Tian, M. Du, L. Qu, S. Chen, S. Zhu and G. Han, *Rsc Advances*, 2017, **7**, 42641-42652.
20. Y.-H. Yu, C.-C. M. Ma, C.-C. Teng, Y.-L. Huang, S.-H. Lee, I. Wang and M.-H. Wei, *Mater Chem Phys*, 2012, **136**, 334-340.
21. K. J. Ji, H. H. Zhao, J. Zhang, J. Chen and Z. D. Dai, *Appl Surf Sci*, 2014, **311**, 351-356.
22. W. L. Song, X. T. Guan, L. Z. Fan, W. Q. Cao, C. Y. Wang, Q. L. Zhao and M. S. Cao, *J Mater Chem A*, 2015, **3**, 2097-2107.
23. P. Ghosh and A. Chakrabarti, *European Polymer Journal*, 2000, **36**, 1043-1054.
24. N. Agnihotri, K. Chakrabarti and A. De, *Rsc Adv*, 2015, **5**, 43765-43771.
25. B. Shen, W. Zhai, M. Tao, J. Ling and W. Zheng, *Acs Appl Mater Inter*, 2013, **5**, 11383-11391.
26. D. X. Yan, P. G. Ren, H. Pang, Q. Fu, M. B. Yang and Z. M. Li, *J Mater Chem*, 2012, **22**, 18772-18774.
27. J. S. Kang, J. Ryu, H. S. Kim and H. T. Hahn, *J Electron Mater*, 2011, **40**, 2268-2277.
28. H. W. Ott, *Electromagnetic compatibility engineering*, John Wiley & Sons, 2011.
29. M. Koledintseva, P. C. Ravva, R. DuBroff, J. Drewniak, K. Rosanov and B. Archambeault, 2005, **1**, 169-174.
30. N. Hu, *COMPOSITES AND THEIR PROPERTIES* 2012.
31. D. X. Yan, H. Pang, B. Li, R. Vajtai, L. Xu, P. G. Ren, J. H. Wang and Z. M. Li, *Advanced Functional Materials*, 2015, **25**, 559-566.
32. S. P. Pawar, S. Biswas, G. P. Kar and S. Bose, *Polymer*, 2016, **84**, 398-419.
33. A. Ameli, M. Nofar, S. Wang and C. B. Park, *Acs Appl Mater Inter*, 2014, **6**, 11091-11100.
34. H. Ji, R. Zhao, N. Zhang, C. Jin, X. Lu and C. Wang, *Npg Asia Mater*, 2018, **10**, 749.
35. V. B. Nam, J. Shin, Y. Yoon, T. T. Giang, J. Kwon, Y. D. Suh, J. Yeo, S. Hong, S. H. Ko and D. Lee, *Advanced Functional Materials*, 2019, **29**.
36. A. Reale, L. La Notte, L. Salamandra, G. Polino, G. Susanna, T. M. Brown, F. Brunetti and A. Di Carlo, *Energy Technol-Ger*, 2015, **3**, 385-406.
37. S. Deb and S.-C. Yao, *International Journal of Heat and Mass Transfer*, 1989, **32**, 2099-2112.
38. A. Jain and S. K. Tripathi, *Journal of Energy Storage*, 2015, **4**, 121-127.
39. M. Vanaja and G. Annadurai, *Applied Nanoscience*, 2013, **3**, 217-223.
40. S. Pande, A. Chaudhary, D. Patel, B. P. Singh and R. B. Mathur, *Rsc Adv*, 2014, **4**, 13839-13849.
41. Y. Li, X. Pei, B. Shen, W. Zhai, L. Zhang and W. Zheng, *Rsc Adv*, 2015, **5**, 24342-24351.
42. P. Cataldi, J. A. Heredia-Guerrero, S. Guzman-Puyol, L. Ceseracciu, L. La Notte, A. Reale, J. Ren, Y. Zhang, L. Liu, M. Miscuglio, P. Savi, S. Piazza, M. Duocastella, G. Perotto, A. Athanassiou and I. S. Bayer, *Advanced Sustainable Systems*, 2018, **2**, 1800069.
43. C. E. K. Mees, *J Soc Motion Pic Eng*, 1941, **37**, 10-21.
44. F. C. Krebs, J. Alstrup, H. Spanggaard, K. Larsen and E. Kold, *Sol Energ Mat Sol C*, 2004, **83**, 293-300.
45. D. D. L. Chung, *Carbon*, 2001, **39**, 279-285.
46. M. Arjmand, T. Apperley, M. Okoniewski and U. Sundararaj, *Carbon*, 2012, **50**, 5126-5134.
47. J. J. Ma, K. Wang and M. S. Zhan, *Rsc Adv*, 2015, **5**, 65283-65296.
48. C. Wan and J. Li, *Carbohyd Polym*, 2016, **150**, 172-179.
49. Y. Wu, Z. Wang, X. Liu, X. Shen, Q. Zheng, Q. Xue and J.-K. Kim, *Acs Appl Mater Inter*, 2017, **9**, 9059-9069.
50. N. Zhang, R. Zhao, D. Y. He, Y. Y. Ma, J. Qiu, C. X. Jin and C. Wang, *Journal of Alloys and Compounds*, 2019, **784**, 244-255.
51. X. Sun, X. Liu, X. Shen, Y. Wu, Z. Wang and J.-K. Kim, *Composites Part A: Applied Science and Manufacturing*, 2016, **85**, 199-206.
52. X. Zhang, S. Jiang, M. Cai, H. Zhao, F. Pan, D. Miao and X. Ning, *Ceramics International*, 2020.

53. M. Montazer and V. Allahyarzadeh, *Industrial & Engineering Chemistry Research*, 2013, **52**, 8436-8444.

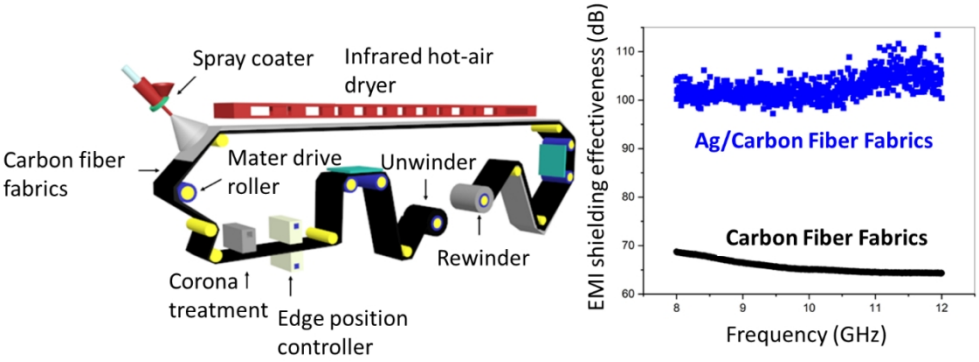
Spray coater
Infrared hot-air dryer
Carbon fiber fabrics
Mater drive roller
Unwinder
Rewinder
Corona treatment
Edge position controller
EMI shielding effectiveness (dB)
Ag/Carbon Fiber Fabrics
Carbon Fiber Fabrics
Frequency (GHz)

Highlight sentence (20 words limit):

Continuous and scalable fabrication of silver coated carbon fiber fabrics with exceptional EMI shielding effectiveness via roll-to-roll spray coating process